iScience

CellPress
OPEN ACCESS

Review

Surface-Plasmon Holography

Satoshi Kawata[1,*] and Miyu Ozaki[2]

SUMMARY

Holography was originally invented for the purpose of magnifying electron microscopic images without spherical aberration and has been applied to photography for recording and reconstructing three-dimensional objects. Although it has been attracting scientists and ordinary people in the world, it is still a technology in science fiction movies. In this review, we discuss a new version of holography that uses surface plasmons on thin metal film. We discuss conventional holography and its drawbacks, such as overlapping of ghost and background due to the contribution of unnecessary diffraction and monochromacy for avoiding the unwanted diffraction components of different colors. Surface-plasmon holography is a version of near-field holography to overcome drawbacks of conventional holography. Comparison with conventional and volume holography for color reconstruction is discussed in reciprocal lattice space. Localized mode of surface plasmons and meta-surface holography are also reviewed, and feature perspectives and issues are discussed.

INTRODUCTION

Surface plasmon polaritons have been studied for many years in physics, electrical engineering, materials science, and even chemistry and biology. In 1899, Sommerfeld predicted the existence of surface light traveling along the metal wire (Sommerfeld, 1899). It was re-found and used as nano-waveguide light in the 1990s (Takahara et al., 1997). A bundle of metallic waveguides was used as a diffraction-free nano-lens in the 2000s (Ono et al., 2005; Kawata et al., 2008). Apart from this story, an optical scientist Robert Wood observed a plasmonic resonance phenomenon when he did an experiment of light diffraction at metallic grating in 1902 (Wood, 1902). The phenomenon was observed as a dark band in a rainbow spectrum. Such a dark band would not have been seen in the ordinary condition of grating alignment, except when the grating surface was accidentally wet with liquid. It was caused by the light absorption of high-order diffraction, due to the coupling of evanescent waves to the surface plasmons. This mechanism was explained much later (Fano, 1941). An optical geometry composed of a high-index prism and a metal plate with a small gap was proposed by Otto for the purpose of excitation of surface plasmons on metal surface (Otto, 1968). This geometry was modified to the one in which thin metal film was physically in contact with the prism to excite surface plasmons on the metal-film surface on the other side of prism (Kretschmann and Raether, 1968). This configuration has been applied to a bio-molecular sensor, named surface-plasmon resonance (SPR) sensor (Nylander et al., 1982; Matsubara et al., 1988a, 1988b), which has detected molecules or liquid due to the index change contact with the metal. In this article, we review the studies on the applications of surface plasmons to holographic display.

Besides the propagating mode of surface plasmons, the localized mode of surface plasmons has also been thoroughly studied. Such a mode has been known as the mechanism producing never-fading beautiful color of stained glass, which comes from metallic nanoparticles dispersed in glass (for example, Maier and Atwater, 2005). The spectroscopy of metallic nanoparticles in dielectrics was reported in 1904 by Maxwell-Garnett (1904). The resonance of localized mode plasmons found many applications, including the enhancement of Raman scattering at molecules (Fleischmann et al., 1974), super-resolving optical microscopy (Inouye and Kawata, 1994; Kawata et al., 2009), tip-enhanced Raman scattering microscopy (Inouye et al., 1999; Hayazawa et al., 2000; Stöckle et al., 2000), nanoparticle lasers or SPASERS (Bergman and Stockman, 2003), cancer treatment (O'Neal et al., 2004), and photovoltaics (Ferry, 2008). The localized mode of surface plasmons has been also applied to holography, which we discuss in this review as well.

We first discuss why and how surface plasmons have been applied to the holographic display. Holography was originally invented by Dennis Gabor as a lensless electron microscope, which did not suffer from the

[1]Department of Applied Physics, Osaka University, Suita, Osaka 565-0871, Japan

[2]Department of Mechanical Engineering, Nippon Institute of Technology, Miyashiro-machi, Saitama, 345-8501 Japan

*Correspondence: kawata@serendipresearch.org

https://doi.org/10.1016/j.isci.2020.101879

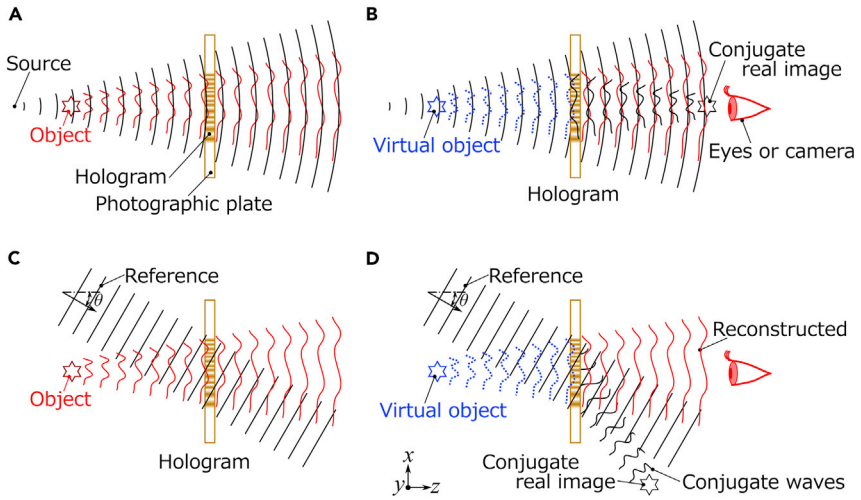

Figure 1. Principle of Hologram Recording and Reconstruction

(A) Recording of Gabor's in-line hologram. A portion of illumination light is diffracted at the object to produce secondary waves. The waves diffracted at the object interfere with non-diffracted waves on the photographic plate to be the hologram.

(B) Reconstruction of Gabor's hologram. The hologram is illuminated by the light in the same optics as that for recording (wavelength may be different). The illumination light and the conjugate component of diffraction overlap as background and ghost in observing the virtual object.

(C) Hologram recording with an off-axial reference beam. A coherent light beam is divided into two: one directly illuminates the photographic plate (reference beam) and the other scatters at the object (this beam is omitted in the figure for simplicity, but it is given from top right). The interference between the reference beam and the scattered beam at the object is recorded on a photographic plate as a hologram.

(D) Reconstruction of a virtual object from the off-axial hologram. The hologram is illuminated by the reference beam. The reference beam and the conjugate component of diffraction are angularly separated from the reconstruction beam (in red). Note that the waves of dashed blue lines in (B) and (D) are virtual.

spherical aberration caused by the electromagnetic lens that inherently limited the spatial resolution (Gabor, 1948, 1949). In addition, Gabor's holography gains a magnification of, for example, 1,000×, because reconstruction is made by light with wavelength 1,000 times longer than that of electron beam for recording. This work was awarded a Nobel Prize for "the invention and development of recording and reconstruction of three-dimensional light field" and attracted optical scientists and photographers. However, it still contains some problems for practical uses as a virtual display. A number of attempts have been made to solve the problems, such as separation of ghost images caused by unnecessary orders of diffraction (Leith and Upatnieks, 1964), elimination of the ghost caused by wrong colors for white-light illumination (Denisyuk, 1962; Benton, 1969, 1977), and near-field recording and reconstruction of hologram (Stetson, 1967; Nassenstein, 1968; Bryngdahl, 1969) for burying unwanted order of diffractions along the grating as near-field evanescent light.

ELIMINATION OF GHOSTS AND BACKGROUND

In-Line and Off-Axis Holography

In Gabor's holography, the interference between the waves from a point source (black waves in Figure 1A) and the waves scattered at the object (red waves in Figure 1A) are recorded on a photographic plate. After the development of photographic plate (hologram), it is placed at the original location in the same optics without object. And then, the hologram is illuminated by a laser, to generate the waves of scattering at the object (red in Figure 1B) in the recording. As a result, the object is seen virtually at its original position (blue star in Figure 1B) by eyes. The conjugate component (black star) and 0th-order diffraction (diverging waves) overlap the reconstruction waves. Those unwanted diffraction components can be separated by dividing the illuminating beam into two with angle: one for illuminating the object and the other for directly illuminating the photographic film (Reference) as shown in Figure 1C (Leith and Upatnieks, 1964). The beam to illuminate the object is omitted in this figure for simplicity. At the hologram plane, light intensity I at position (x, y) is given by the complex amplitude of reference waves $r(x,y)$ and that of scattering ones $o(x,y)$ as

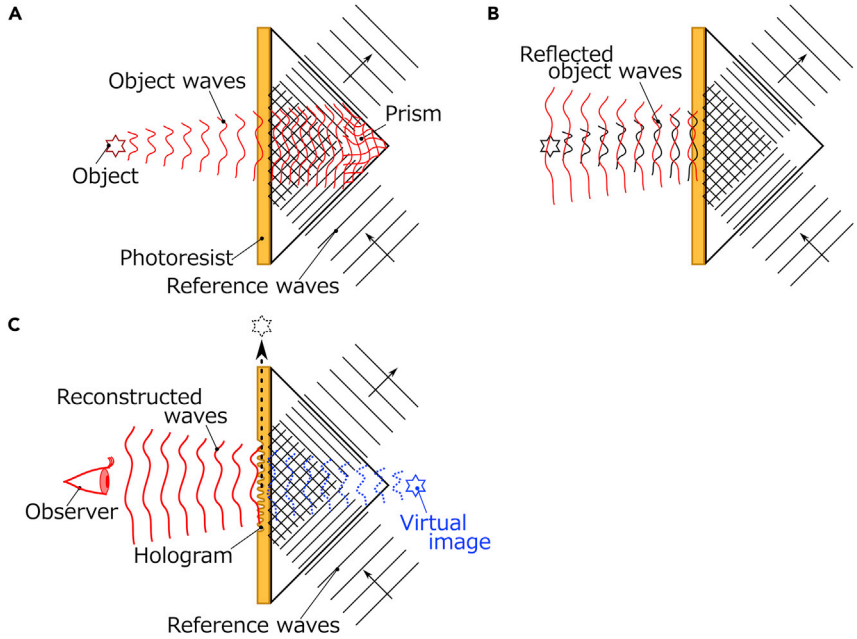

Figure 2. Evanescent-Wave Holography

(A) Recording configuration. The reference beam becomes evanescent waves on the high-index prism by total internal reflection. The interference between the reference beam and the scattered light at the object is recorded on the photoresist.

(B) Due to the large index difference between the prism and air, the scattering light reflects back toward the object side.

(C) Reconstruction of the object from the evanescent-wave hologram. The observer stands at the side where the object was placed in recording while the object is virtually observed through the hologram. The background light reflects back to the prism side due to the total internal reflection. Any ghost or conjugate component does not emit out from the hologram plane but exists as evanescent waves.

$$I = (r + o)(r + o)^* = |r|^2 + |o|^2 + r^*o + ro^* \quad \text{(Equation 1)}$$

where * indicates complex conjugate. In the reconstruction, the hologram (assumed to be recorded in a positive film) is illuminated by reference beam r, i.e.,

$$rI = r(|r|^2 + |o|^2) + |r|^2 o + r^2 o^*. \quad \text{(Equation 2)}$$

If the intensity of reference beam is uniform in x and y, this reduces to

$$rI = r(1 + |o|^2) + o + r^2 o^*. \quad \text{(Equation 3)}$$

Here, object $o(x,y)$ is found as the second component of the right side of the equation, representing the reconstruction of the virtual object. The first component $r(1 + |o|^2)$ represents propagating waves of reference (plane waves in black in Figure 1D), and the third component $r^2 o^*$ represents conjugate waves o^* to image the object in the observation space in reconstruction. Due to the multiplication by r^2 this component does not overlap but separates from the object wave o in reconstruction (Figure 1D).

Evanescent Wave Holography: Confined Light Waves on the Surface

Although the ghost and background have been separated from the waves of the virtual object in off-axial holography, they still exist in the side where the eye or a camera is set, as shown in Figure 1D. These unwanted components can be removed from the observation by using near-field light or evanescent waves. Evanescent-wave holograms were developed by Nassenstein and Bryngdahl independently in 1968 (Nassenstein, 1968; Bryngdahl, 1969).

Figure 2A shows a typical configuration of evanescent-wave holography, where the reference beam is converted to the evanescent waves by total internal reflection at the surface of a high-index prism. The light

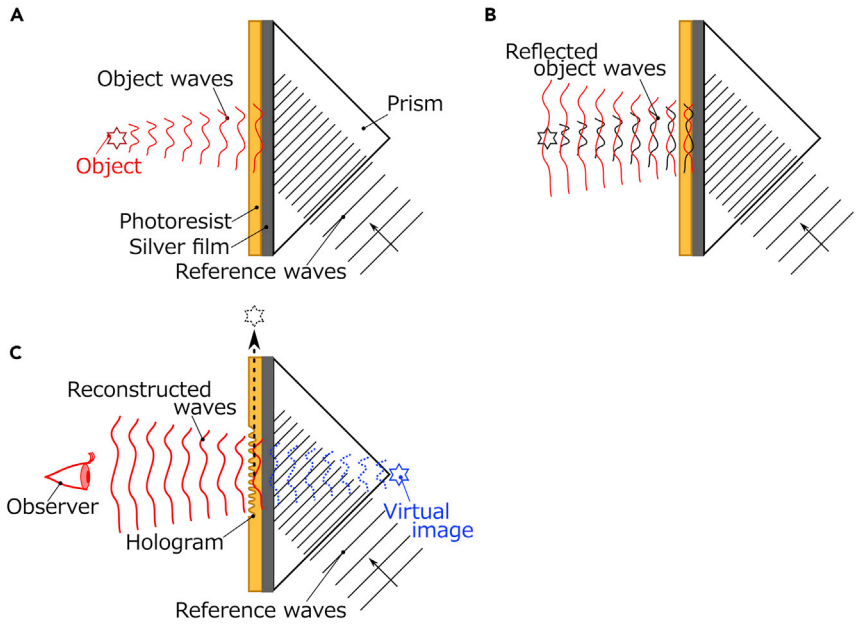

Figure 3. Surface-Plasmon Holography.

This is the same as evanescent-wave holography except that a thin metal film is sandwiched between the prism and photographic film (hologram).

(A) Recording configuration. Compared with the evanescent-wave holography, there is no stray light in the prism side, which deteriorates the hologram pattern.

(B) The scattered light reflects back toward the object side at the metal film.

(C) Reconstruction of the object. An observer sees the object virtually in the prism. If no light illuminates the hologram, the metal film works as a mirror.

scattered at the object reaches the photographic film (or photo-resist) on the prism to interfere with the reference beam forming evanescent waves on the prism surface (not shown in the figure). The light illuminating the object and the reference beam originally come from the same light source but are divided into two. The object-scattered waves (marked in red) propagate through the prism and distort themselves due to the high index of the prism and the reflection at the prism edges. In addition, the object-scattered light reaching the photographic film reflects back due to the index difference between the free space (air) and the high-index prism as shown in Figure 2B. In reconstruction, the observer on the object side (free space) sees the object virtually in the prism side (Figure 2C).

Here, it is to be noted that the conjugate component is trapped in the hologram plane as evanescent waves. As a result, no ghost or background light deteriorates the holographic reconstruction. In addition, there is no light source or beam path in the observer side. The observer does not physically block the light path, which usually happens for the conventional reflection-type holography. The use of a planar waveguide or a light guide as a substitute of high-index prism makes this hologram system very compact (Lukosz and Wüthrich, 1976; Suhara et al., 1976).

Surface-Plasmon Holography: Reconstruction from Opaque Film

If a metallic film is coated on the prism surface under the hologram (photoresist) in the evanescent holography configuration (Figure 3A), surface plasmons can be localized on the thin hologram when the condition of SPR is satisfied by choosing incident angle and laser wavelength for illumination. Figures 3A and 3B show the configurations of recording and reconstruction for plasmon holography (Cowan, 1980). Silver and gold are typical plasmonic metals with a film thickness of 30–50 nm (Raether, 1988; Kawata, 2013).

In the recording system, the waves scattered at the object reflect at metal film and do not penetrate into the prism (Figure 3A), so that no stray light travels in the prism differently from the hologram. As a result, surface-plasmon holography is free from the ghost due to the stray light in recording (compare with Figure 2A). In surface-plasmon holography, the reflection of object waves at metal film is recorded as a hologram

(Figure 3B). The observer standing in the object side (free space) sees the virtual object in the prism side in reconstruction (Figure 3C). When illumination light is off, the thin metal film works as a reflection mirror, whereas the virtual object appears behind the hologram when light is on.

The reference beam can also be given from the air side rather than from the prism side to record a hologram (Maruo et al., 1997). In this case, the size and the position of the virtual object in reconstruction differ from those of the original object. Figure 4 shows an example of reconstructed image set of surface-plasmon holography (Maruo et al., 1997). A planar waveguide and a light guide have been also used for surface-plasmon holography (Wang et al., 2001).

COLOR REPRESENTATION

Raman-Nath Diffraction and Bragg Diffraction

For reconstructing an object in color from a hologram, light with three colors (red, green, and blue) or white light is necessary. Figure 5A shows the reconstruction optics of Leith-Upatnieks's hologram (a simple grating for the sake of simplicity) illuminated in three colors. Three color light reconstructs three virtual objects in different angles from the hologram, each in a different color. In Gabor's holography, three objects are reconstructed at three different magnifications each in a different color. In both configurations, only one image in reconstruction is the true virtual object, whereas the other two are the false images to overlap the true one.

The generation of false images in wrong colors is explained in the reciprocal lattice space with use of Ewald sphere, which is known in crystallography. Figure 5B shows Ewald spheres (circles in the figure) for blue and red lights; light wavevectors K_i and K_d of incidence and diffraction, respectively; and the grating vector K_g. This hologram is assumed to be pre-recorded by blue light, so that in reconstruction blue-light with wavevectors K_i for illuminating the hologram with grating vector K_g generates diffraction K_d on the Ewald sphere to form a closed triangle. For red light illumination, these three vectors do not form a closed triangle. Nevertheless, if the hologram is thin enough, the red light may diffract by the grating made in blue. Such diffraction is called as Raman-Nath diffraction. If the hologram is thin, the grating vector K_g is not defined as a line in a given direction but the line end fans out in the reciprocal lattice space (a black line perpendicular to the arrow K_g at the end in Figure 5B). As a result, false color images of the object emerge from a thin hologram.

If a hologram is thick enough (Figure 5C), only a selected wavelength of light (blue in Figure 5C) diffracts at the hologram, and light of other wavelengths transmit through the grating. Such a thick hologram was invented by Denisyuk (1962) and was called a volume hologram. Figure 5D shows the mechanism of volume holography in the reciprocal lattice space. Differently from Figure 5B, the grating vector K_g of a thick grating does not fan, so that the diffraction of the wrong color (in red) by the grating K_g recorded in blue does not couple with red light K_d on the Ewald sphere in any angle. Such diffraction by the thick grating is called Bragg diffraction.

Surface Plasmons for Color Holography

Although Denisyuk's volume holography has a great potential for practical applications, it has been limited in its applicability due to the durability and the lifetime of materials. On the contrary, thin holograms are durable, whereas not applicable to color representation with white light as discussed above, because they are Raman-Nath diffraction based. The authors have reported the use of surface plasmons for color holography with white light illumination (Ozaki et al., 2011). The mechanism originated from Wood's finding of anomaly in grating diffraction (Wood, 1902) and SPR sensors for ultra-sensitive molecular sensing (Nylander et al., 1982; Matsubara et al., 1988a; 1988b).

Surface-plasmon holography has been explained already in the previous section from the viewpoint of the suppression of conjugate image and background. In this section, we discuss it as color holography. Even though surface-plasmon holography is classified in Raman-Nath-based thin-film holography, the false-color components disappear in reconstruction (Figure 5E). This can be explained with the dispersion relationship of surface plasmons (Figure 5F). The dispersion curve of surface plasmon asymptotically reaches SPR ω_{sp} of the metal in contact with the hologram. Light propagating in the air cannot couple with surface plasmons because the dispersion curve of light (a straight line in Figure 5F) does not cross or meet that of surface plasmons (a curve in Figure 5F). If the light is in a high-index prism, it reduces the speed (the angle of

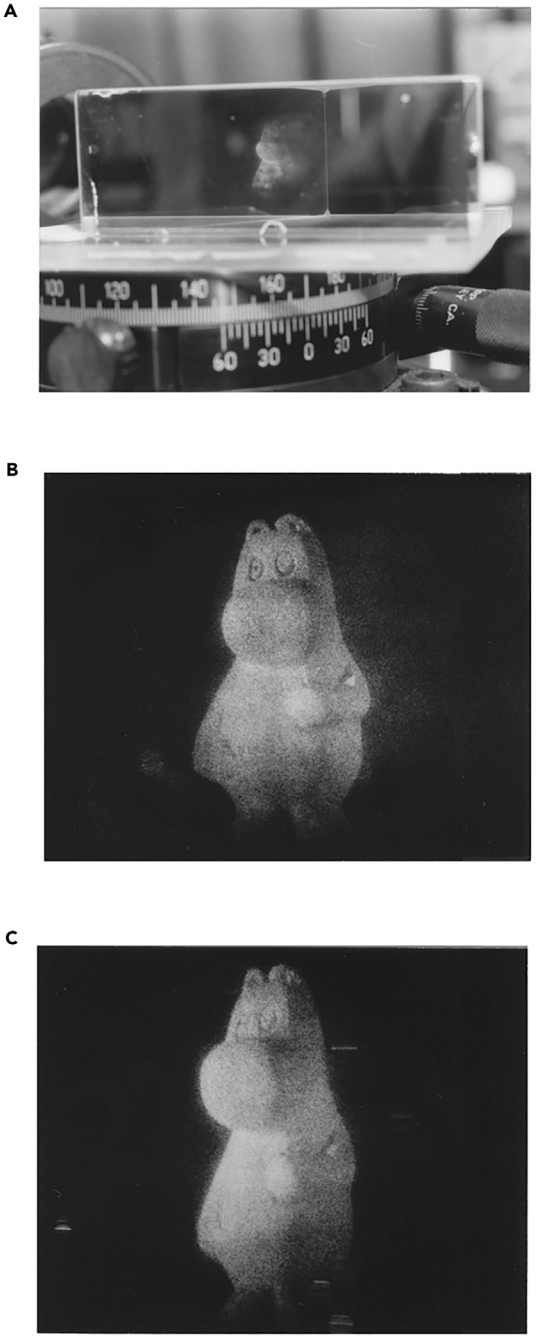

Figure 4. Example of Three-Dimensional Object Reconstruction from a Surface-Plasmon Hologram
(A) The reconstructed object is seen through the metal film on the prism in a distance.
(B and C) Enlarged views at different view angles
Reprinted with permission from (Maruo et al., 1997). © The Optical Society.

light line becomes smaller in Figure 5F), and hence the light may couple with surface plasmons. The coupling occurs only at a selected color, for example, blue light at ω_{blue} in Figure 5F, the wavenumber k_{izBlue} of which (more precisely, z component of incident light k_i) is the same as that of surface plasmons k_{spBlue}, i.e., $K_{izBlue} = K_{spBlue}$. Other color light, for example, red light at ω_{red} does not couple with plasmons, or $K_{izRed} \neq K_{spRed}$. As a result, surface plasmons select a color from white light for reconstruction.

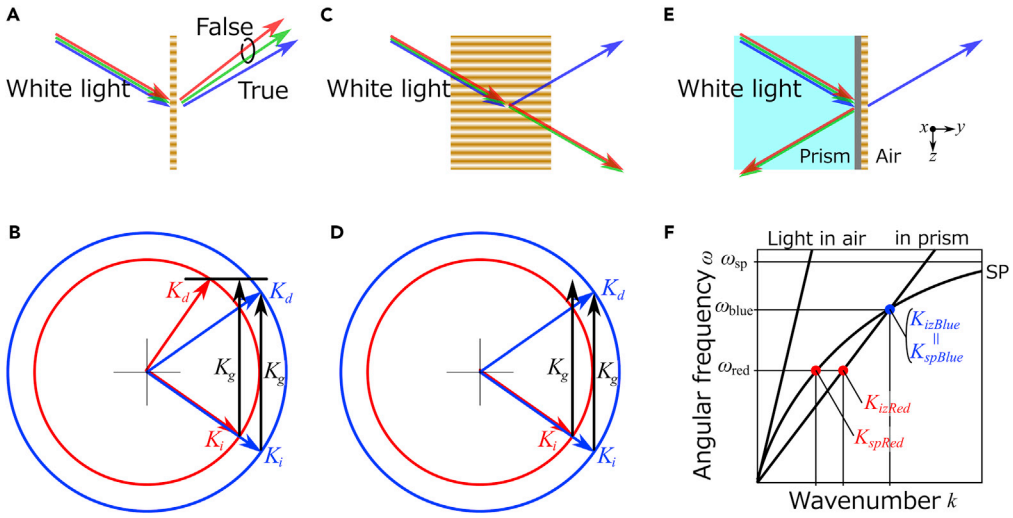

Figure 5. Holography Based on Raman-Nath and Bragg Diffractions

(A) Conventional thin-film holography. Hologram reconstruction is based on Raman-Nath diffraction. White light illumination (in the figure, three colors) onto the hologram produces reconstruction of waves in different angles, resulting in false images in the wrong colors.

(B) Raman-Nath diffraction with use of Ewald sphere. For the thin-film hologram geometry, not only the light of the wavelength satisfying Bragg diffraction condition (blue in the figure) but also the light of other wavelengths (for example, red in the figure) diffracts by the hologram, because grating vector k_g of hologram fans at its end (black line).

(C) Denisyuk's volume holography. Only a selected-color light (in figure blue one) is diffracted at the hologram.

(D) Bragg diffraction for a thick hologram with use of Ewald sphere. Same as (B) except that only the wavelength component satisfying Bragg diffraction diffracts, otherwise not.

(E) Surface-plasmon holography. Only a selected wavelength component excites surface plasmons on the metallic film to reconstruct the recorded waves by the thin hologram (grating in the figure) to the far field.

(F) Explanation of plasmon coupling with use of ω-k dispersion curve. The light line in prism meets the curve of surface plasmons, which asymptotically reaches the surface-plasmon resonance ω_{sp} on the surface of the metal in contact to the hologram. This coupling occurs at a selected wavelength light (in this example, blue) as $K_{izBlue} = K_{spBlue}$, but not other wavelengths, for example, $K_{izRed} \neq K_{spRed}$.

More precisely, wavenumber k_{sp} of surface plasmons propagating on the metal surface is given by

$$k_{sp} = \frac{\omega}{c}\left(\frac{n_h^2\, n_m(\omega)^2}{n_h^2 + n_m(\omega)^2}\right) \qquad \text{(Equation 4)}$$

where ω and c are the angular frequency and the speed of light in vacuum, respectively, and n_h, and n_m are the refractive indices of hologram media and metal, respectively (Raether, 1988). For simplicity, we discuss only the real part of refractive index, although n_m should be complex. n_m varies as a function of ω as $n_m(\omega)$.

For reconstructing a surface-plasmon hologram, the light is incident onto the metal film through the prism, and is converted to the evanescent waves to propagate along the metal film surface. The z component of wavenumber k_{iz} of evanescent waves along the metal film is expressed as

$$k_{iz} = \frac{\omega}{c} n_g \sin\theta \qquad \text{(Equation 5)}$$

where n_g is the refractive index of prism and θ is the incident angle.

The coupling between light (evanescent waves) and surface plasmons occurs only at the frequency at which z component of wavenumber is common to both. The configuration of surface-plasmon holography proposed by the authors is shown in Figure 6A, where a white light illuminates a hologram at three different angles (θ and ϕ). A virtual object is reconstructed in color (red, green and blue). As discussed above, due to the plasmon resonance at the selected wavelength, no ghost image with wrong color appears. To enhance the spectral separation in reconstruction, high-index material (SiO_2) is coated on the hologram (the upper part of Figure 6B) to increase the effective index n_h in Equation (4) (Ozaki et al., 2013). The lower part of Figure 6B shows the enhancement effect of spectral separation. In the recording step, the

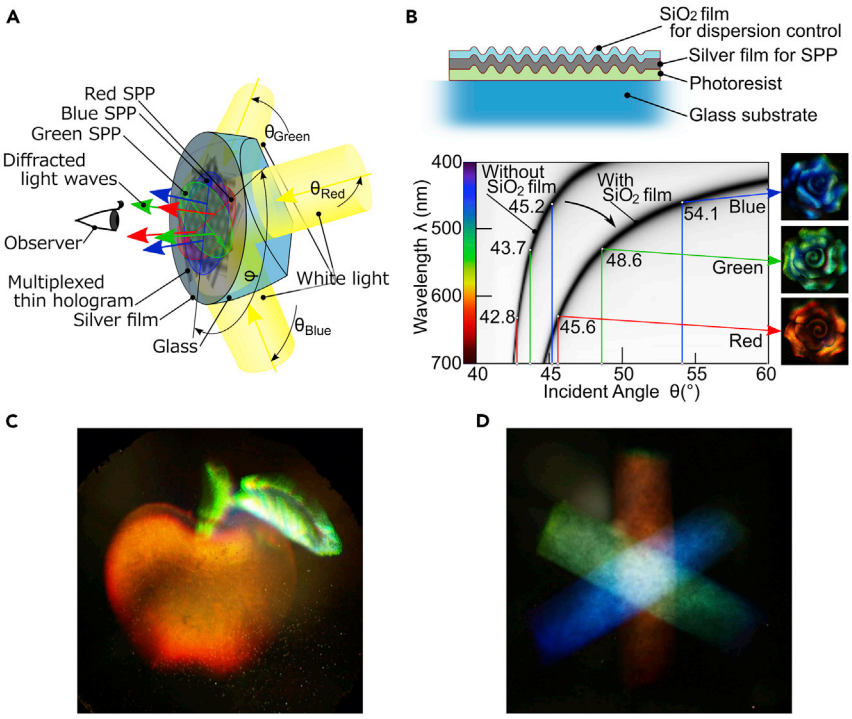

Figure 6. Surface-Plasmon Holography

(A) Configuration of reconstruction optics for a color object from a plasmon hologram. White light is introduced from three positions in different angles (θ and ϕ) to reconstruct a virtual object in color.

(B) Plasmon hologram (corrugated metallic thin film) is sandwiched by dielectric photoresist hologram and high-index (SiO_2) thin film. Plasmon hologram follows the surface corrugation of photoresist hologram on the glass substrate. SiO_2 film works for enhancing the color separation as shown in the dispersion curve in the lower part.

(C) An experimental example of a three-dimensional color object reconstructed from a surface-plasmon hologram. A red apple with a green leaf is well reconstructed in three dimensions at different viewing angles.

(D) Color balance test with red, green, and blue by rotating the bar by 120° for each color. In the center, where the three colors overlap, a hexagonal area is reconstructed as white, whereas yellow triangles are reconstructed where red and green overlap.

From (Ozaki et al., 2011). Reprinted with permission from AAAS.

interference between object-scattered light and reference beam is exposed on photoresist film on the glass substrate to produce a surface-relief hologram, and then silver film is coated on the surface of the photoresist, resulting in a metallic plasmon hologram. SiO_2 film is then coated on the plasmon hologram by evaporation.

Figure 6C shows an experimental example of a three-dimensional reconstruction of an apple in color from a surface-plasmon hologram. A color object (in red, green, and blue) is observable in three dimensions by changing the viewing angle and viewing position (a movie in color is found in the article by Ozaki et al. (2011). A halogen lamp was used for reconstruction. Figure 6D shows an image of a bar taken by three-time exposure in R, G, and B to prove a good white-color balance.

Another version called a rainbow hologram, invented by Benton (1969), is also based on Raman-Nath diffraction, but does not suffer from the overlapping by unwanted color images for white-light reconstruction. Rainbow holograms have been successfully and widely used in credit cards as security codes. However, a rainbow hologram does not reconstruct a full (true) color object; a single-color image appears at a given viewing angle, and the color changes by rotating the hologram or by changing the viewing angle.

CATEGORIZATION OF NEAR-FIELD HOLOGRAPHY

Here we summarize different versions of near-field optical holography including surface-plasmon holography and evanescent holography, in terms of structures, mechanisms, and functions (Table 1). They are

Structures	Mechanism/Functions	Authors/Inventors, Years
Non-plasmonic		
High-index prism	• Total internal reflection • Background/ghost free	Stetson, 1967 Nassenstein, 1968 Bryngdahl, 1969
Planer dielectric waveguide	• Waveguide mode • Background/ghost free • Small and thin	Lukosz and Wüthrich, 1976 Suhara et al., 1976
Plasmonic		
Metal film on high-index prism (Figure 7A)	• Plasmon excitation with Kretschman's configuration • No stray light • Works as a mirror when no illumination	Cowan, 1980 Maruo et al., 1997
Planar waveguide on metal film on prism	• Waveguide mode • Plasmon resonance is not necessary	Wang et al., 2001
Metal film hologram (Figure 7B)	• Uniform thickness of metal film • SPP (surface plasmon polaritons) excitation is spatially uniformed • The first report of plasmonic color hologram with white light illumination	Ozaki et al., 2011
Metal grating (Figure 7C)	• The first report on plasmonic hologram • Unwanted diffractions appear and overlap the virtual object image	Cowan, 1972 Cowan, 1974

Table 1. Near Field Holography

categorized into non-plasmonic and plasmonic ones. Non-plasmonic holography based on total internal reflection with high-refractive-index material was reported in the 1960s (Stetson, 1967; Nassenstein, 1968; Bryngdahl, 1969) and with planar dielectric waveguides in the 1970s (Lukosz and Wüthrich, 1976; Suhara et al., 1976). In this type, holograms are placed in the near field of the prism or the planar waveguide, and ghost and background are not seen in the far field.

The surface-plasmon holography was first reported by Cowan in 1980 (Cowan, 1980), where a metal film is sandwiched between the hologram and a high-index prism (Figure 7A), so that it looks like a reflecting mirror when illumination light from the back is off (Maruo et al., 1997). The waveguide mode in the dielectric film coated on the metal can be used as reference light, where plasmonic resonance is not necessary for hologram recording or reconstruction (Wang et al., 2001).

Another configuration of surface-plasmon hologram is shown in Figure 7B, where metallic thin film and dielectric hologram are combined into one. The hologram is optically recorded on the photoresist film to form corrugation (height distribution) rather than density (index) distribution, and metal film is coated on it, following the surface corrugation of photoresist as a template. As a result, metallic film is corrugated

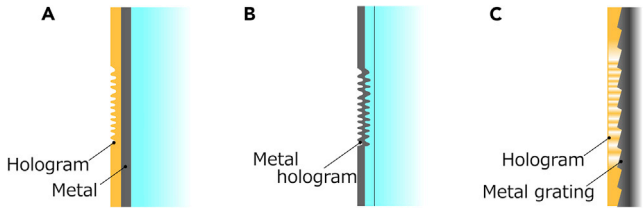

Figure 7. Layer Configuration of Surface-Plasmon Holograms

(A) Dielectric (photoresist) hologram is on the plasmonic thin-metal film on which surface plasmons are excited. (B and C) (B) A plasmonic thin-metal hologram is on the dielectric substrate with corrugation. (C) Hologram on a metal grating. Surface plasmons are excited on the metal grating and diffracted by the hologram.

as a metallic hologram (Ozaki et al., 2011). Blurring of an image due to the extended light source can also be suppressed with use of surface plasmons (Ozaki et al., 2012).

A higher order of diffraction of a grating can be also used for generating surface plasmons similarly to the Wood's experiment discussed above (Wood, 1902). It was reported by Cowan in the 1970s (Cowan, 1972, 1974). In this configuration (Figure 7C), the hologram was photographic emulsion coated on the aluminum-coated diffraction grating. As this configuration contains two gratings (hologram itself and the grating to generate plasmons), unnecessary diffraction components by the coupling due to two gratings are generated, which contribute as ghost images to overlap with the reconstructed virtual image.

LOCALIZED PLASMONS AND METASURFACE HOLOGRAMS

Besides the surface-plasmon holography based on propagating surface plasmons, there have been reports on holography with use of localized-mode surface plasmons. Localized-mode surface plasmons are the standing waves of surface plasmons at a finite length of metal as Fabry-Perot interferometer of surface plasmons. As metal absorbs plasmons, Q factor of the resonance modes of this interferometer is low, so that the peaks of modes are broad, typically ~100 nm in wavelength spectrum (Sun and Xia, 2003). A variety of metallic nanoparticles have been proposed to excite localized modes. Among them, metallic V- or C-shaped nanostructures are of interest, because they work as sprit ring resonators to induce negative magnetic field in response to the electromagnetic (light) field at a given frequency. Electromagnetic induction in a three-dimensional array of nano-sprit ring resonators was reported for exhibiting extraordinary and exotic optical properties, such as negative refraction and cloaking, and was named as metamaterials (Smith et al., 2004). A two-dimensional version of metamaterials for hologram application was first reported by Shalaev's group, as a metasurface hologram, where V-shaped nano-antennas were aligned to produce arbitrary phase distribution as desired on the substrate surface by optimizing the orientation and the angle of individual nano-antennas (Ni et al., 2013). Similarly to Fresnel lens, a light beam efficiently refracts by a metasurface hologram to produce a virtual image at some distance from the hologram.

Figure 8 shows an example of metasurface as a metallic V-shaped nano-unit array in line (shown in yellow at the top) and the refracting wavefronts as a function of distance from the array (Yu et al., 2011). Figure 9A shows a holographic reconstruction of 6 letters (8-μm wide for each), observed ~10 μm above the hologram with a microscope objective. A scanning electron microscopic image of a part of the hologram (letter P) is shown in Figure 9B; the lower right inset shows a magnified view of a part of V-shaped unit array (Ni et al., 2013).

Plasmonic nanostructures without the effect of electromagnetic induction have been also reported (Huang et al., 2013), where the phase of unit metallic nano-rod antenna varies as a function of antenna orientation with use of circular polarization. This was also called as metasurface holography (Huang et al., 2018).

Multi-color reconstruction is also possible with localized-mode surface plasmons with different sizes of nanoparticles. Figures 10A and 10B show the schematics and an experimental result of two-color holography (Montelongo et al., 2014). To suppress the unwanted localized mode that scatters the light in a wrong color, a well-designed two-dimensional rod/sphere arrangement of unit cells was proposed

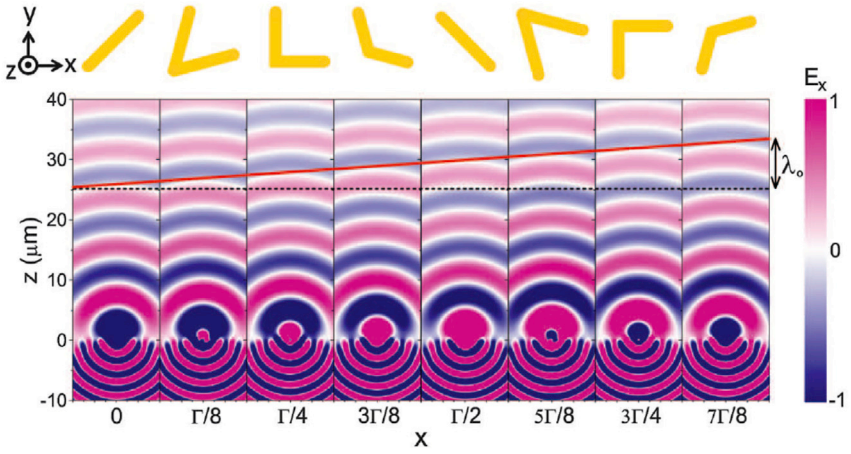

Figure 8. Phase Propagation from Individual V-Shaped Nano-Antenna

The upper images show the array of antennas (x-y) in yellow. A plane wave radiates out from the array (in x) toward z in the direction as designed.

From (Yu et al., 2011). Reprinted with permission from AAAS.

(Figure 10C). Or a hologram can be segmented into small blocks for different colors, each composed of rods of given length (Figure 10D) (Huang et al., 2015), which is equivalent to the painting of blocks in different colors.

The holograms with localized-mode plasmons, whether based on metasurface or non-metasurface, were not recorded optically, but they were fabricated one pixel by one pixel by e-beam (or focused ion beam) lithography, because localized-plasmon structures were too small to record with light. Those holograms were calculated by computer as solutions of inverse scattering problem. The spatial distribution of amplitude and phase at the hologram was calculated by the iterative back-propagation algorithm. The calculation result was printed with metal on the substrate by e-beam. This process took much longer than a real-time optical recording of hologram, and the size of reconstructed virtual object was often too small to seen by the eyes. The optical recording with metallic nanoparticles has been reported with photo-reduction (Sugiyama et al., 2001; Kaneko et al., 2003), photo-migration (Vaia, 2001), and photo-ionization (Akella, 1997), although none of them have been applied to holography.

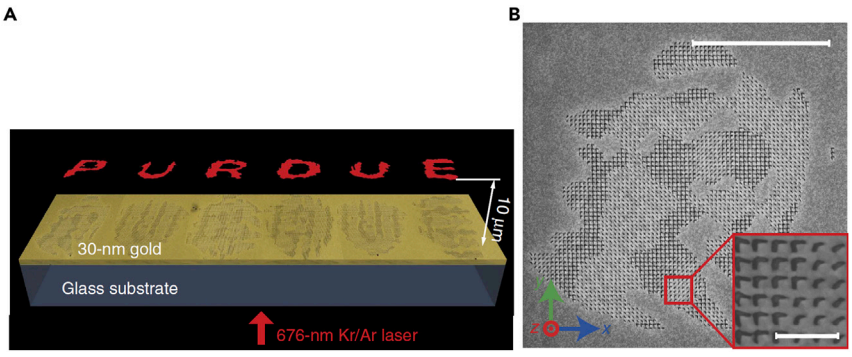

Figure 9. Experimental Result of Reconstruction from a Metasurface Hologram

(A) Schematics of object reconstruction of metasurface hologram. The hologram and the reconstructed virtual object of six letters are both observed with a microscope objective.

(B) Hologram of letter P in (A) observed with a scanning electron microscope. The lower right inset shows a magnified view of a part of the V-shaped unit array. Scale bars, 5 μm (on top) and 500 nm (in inset), respectively.

Reprinted by permission from Springer Nature (Ni et al., 2013).

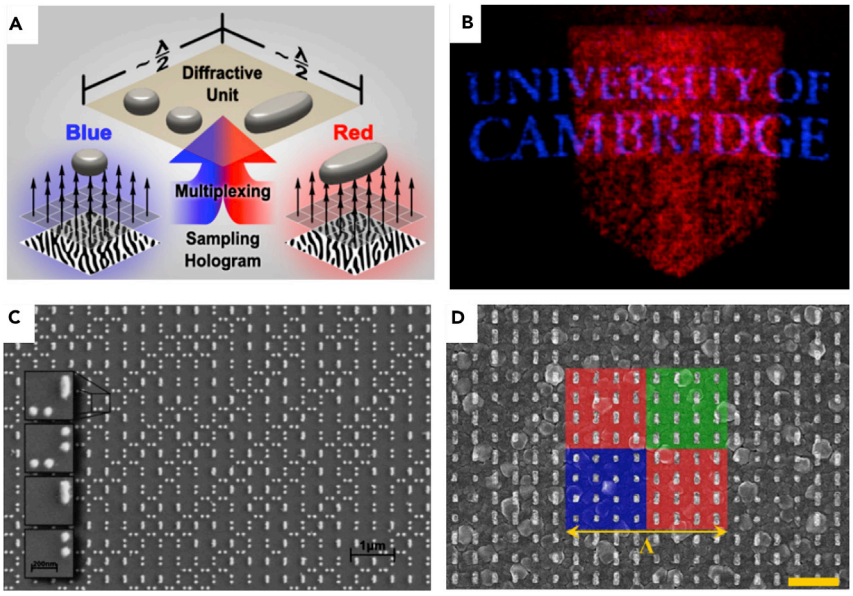

Figure 10. Holography with Localized Modes of Surface Plasmons for Color Reconstruction

(A) A hologram consists of rods of two different lengths to represent two colors. The rod length determines a resonance peak of plasmon frequency.

(B) An experimental result of reconstruction from the hologram depicted in (A).

(C) A scanning electron microscopic image of the hologram illustrated in (A). Plasmonic rods with two lengths are distributed to form a multiplexed hologram of red and blue (Montelongo et al., 2014). Copyright (2014) National Academy of Sciences (A, B, and C).

(D) Another type of color hologram based on localized-mode surface plasmons. The rods of three different lengths representing three different colors (red, green, and blue) are assembled in individual segments. Scale bar, 500 nm. Reprinted with permission from (Huang et al., 2015). Copyright (2015) American Chemical Society.

CONCLUSIONS AND DISCUSSIONS

We reviewed the principles, the functions, the history, and the state of art of surface-plasmon holography and related topics. Surface plasmons add new functions to the conventional holography, such as ghost- and background-free imaging and color representation with white light illumination. Compared with volume holograms, surface-plasmon holograms are made of thin film, based on Raman-Nath diffraction. Surface-plasmon holography removes light sources from the observer's space. Blurring due to the extended light source is also removed due to the narrow incident-angle resonance of surface plasmon. In the review, localized-mode surface plasmons and metasurfaces for the holography application were also reviewed. The principle and mechanism are fundamentally different from those of propagating-mode surface-plasmon holography in terms of recording process and color representation.

Holography has been competing with stereoscopy for three-dimensional viewing, which was invented in the 1830s (Wheatstone, 1838) and has been used for both personal and commercial use. It makes the viewers perceive scenes in three dimensions from two photographs pre-recorded with two cameras at different angles. Compared with the hologram reconstruction, the observers cannot change the viewing position and angle. Stereoscopy principle is now used in movie theaters as 3D cinemas. On the other hand, holography as a virtual movie appears only in the science-fiction movies, but has not been yet commercialized, except a few preliminary trials with a small number of frames as cinematographic holography (Leith et al., 1966; Bitetto, 1968; Yamaguchi et al., 1992). Recently, there was a report on cinematographic holography with metasurface holograms (Izumi et al., 2020).

The number of pixels is still insufficient to record and reconstruct a color movie hologram composed of phase and amplitude distribution in real time even with use of most advanced liquid-crystal spatial light modulators and CCDs. We have to wait for the arrival of further advanced electronics technologies.

ACKNOWLEDGMENTS

The authors started the surface-plasmon holography project when they were in Nanophotonics Laboratory at RIKEN, Japan. They would like to thank RIKEN for the generous support to pursue the project. The project has been done through fruitful discussion with our member Dr. Jun-ichi Kato, who passed away after the two authors left RIKEN. We would like to thank him and appreciate his contribution to this review article.

REFERENCES

Akella, A., Honda, T., Liu, A.Y., and Hesselink, L. (1997). Two-photon holographic recording in aluminosilicate glass containing silver particles. Opt. Lett. *22*, 967–969.

Benton, S.A. (1969). Hologram reconstructions with extended incoherent sources. J. Opt. Soc. Am. *59*, 1545A.

Benton, S.A. (1977). White-light transmission/reflection holographic imaging. In Applications of Holography and Optical Data Processing, E. Marom, A.A. Friesem, and E. Wiener-Avnear, eds. (Pergamon Press), pp. 401–409.

Bergman, D.J., and Stockman, M.I. (2003). Surface plasmon amplification by stimulated emission of radiation: Quantum generation of coherent surface plasmons in nanosystems. Phys. Rev. Lett. *90*, 027402.

Bitetto, D.J.D. (1968). A Holographic motion picture film with constant velocity transport. Appl. Phys. Lett. *12*, 295–297.

Bryngdahl, O. (1969). Holography with evanescent waves. J. Opt. Soc. Am. *59*, 1645–1650.

Cowan, J.J. (1972). The surface plasmon resonance effect in holography. Opt. Commun. *5*, 69–72.

Cowan, J.J. (1974). Holography with standing surface plasma wave. Opt. Commun. *12*, 373–378.

Cowan, J.J. (1980). Surface plasmon holography. AIP Conf. Proc. *65*, 515–518.

Denisyuk, Y.N. (1962). Photographic reconstruction of the optical properties of an object in its own scattered radiation field. Dokl. Phys. *7*, 543–545.

Fano, U. (1941). The theory of anomalous diffraction gratings and of quasi-stationary waves on metallic surfaces (Sommerfeld's waves). J. Opt. Soc. Am. *31*, 213–222.

Ferry, V.E., Sweatlock, L.A., Pacifici, D., and Atwater, H.A. (2008). Plasmonic nanostructure design for efficient light coupling into solar cells. Nano Lett. *8*, 4391–4397.

Fleischmann, M., Hendra, P.J., and McQuillan, A.J. (1974). Raman spectra of pyridine adsorbed at a silver electrode. Chem. Phys. Lett. *26*, 163–166.

Gabor, D. (1948). A new microscopic principle. Nature *161*, 777–778.

Gabor, D. (1949). Microscopy by reconstructed wave-fronts. Proc. Roy. Soc. A. *197*, 454–487.

Hayazawa, N., Inouye, Y., Sekkat, Z., and Kawata, S. (2000). Metallized tip amplification of near-field Raman scattering. Opt. Commun. *183*, 333–336.

Huang, L., Chen, X., Mühlenbernd, H., Zhang, H., Chen, S., Bai, B., Tan, Q., Jin, G., Cheah, K.-W., Qiu, C.-W., et al. (2013). Three-dimensional optical holography using a plasmonic metasurface. Nat. Commun. *4*, 2808.

Huang, Y.-W., Chen, W.T., Tsai, W.-Y., Wu, P.C., Wang, C.-M., Sun, G., and Tsai, D.P. (2015). Aluminum plasmonic multicolor meta-hologram. Nano Lett. *15*, 3122–3127.

Huang, L., Zhang, S., and Zentgraf, T. (2018). Metasurface holography: from fundamentals to applications. Nanophotonics *7*, 1169–1190.

Inouye, Y., and Kawata, S. (1994). Near-field scanning optical microscope with a metallic probe tip. Opt. Lett. *19*, 159–161.

Inouye, Y., Hayazawa, N., Hayashi, K., Sekkat, Z., and Kawata, S. (1999). Near-field scanning optical microscope using a metallized cantilever tip for nanospectroscopy. Proc. SPIE *3791*, 40–48.

Izumi, R., Ikezawa, S., and Iwami, K. (2020). Metasurface holographic movie: a cinematographic approach. Opt. Express *28*, 23761–23770.

Kaneko, K., Sun, H.B., Duan, X.M., and Kawata, S. (2003). Two-photon photoreduction of metallic nanoparticle gratings in a polymer matrix. Appl. Phys. Lett. *83*, 1426–1428.

Kawata, S. (2013). Plasmonics: Future outlook. Jpn. J. Appl. Phys. *52*, 010001, 1–10.

Kawata, S., Ono, A., and Verma, P. (2008). Subwavelength colour imaging with a metallic nanolens. Nat. Photon. *2*, 438–442.

Kawata, S., Inouye, Y., and Verma, P. (2009). Plasmonics for near-field nano-imaging and superlensing. Nat. Photon. *3*, 388–394.

Kretschmann, E., and Raether, H. (1968). Radiative decay of non radiative surface plasmons excited by light. Z. Naturforsch. *23 a*, 2135–2136.

Leith, E.N., and Upatnieks, J. (1964). Wavefront reconstruction with diffused illumination and three-dimensional objects. J. Opt. Soc. Am. *54*, 1295–1301.

Leith, E.N., Upatnieks, J., Kozma, A., and Massey, N. (1966). Hologram visual displays. J. Soc. Motion Pict. Telev. Engrs *75*, 323–326.

Lukosz, W., and Wüthrich, A. (1976). Hologram recording and readout with evanescent field of guided waves. Opt. Commun. *19*, 232–235.

Maier, S.A., and Atwater, H.A. (2005). Plasmonics: Localization and guiding of electromagnetic energy in metal/dielectric structures. J. Appl. Phys. *98*, 011101.

Maruo, S., Nakamura, O., and Kawata, S. (1997). Evanescent-wave holography by use of surface-plasmon resonance. Appl. Opt. *36*, 2343–2346.

Matsubara, K., Kawata, S., and Minami, S. (1988a). A compact surface plasmon resonance sensor for measurement of water in process. Appl. Spectrosc. *42*, 1375–1379.

Matsubara, K., Kawata, S., and Minami, S. (1988b). Optical chemical sensor based on surface plasmon measurement. Appl. Opt. *27*, 1160–1163.

Maxwell Garnett, J.C. (1904). XII. Colours in metal glasses and in metallic films. Phil. Trans. R. Soc. A. *203*, 359–371.

Montelongo, Y., Tenorio-Pearl, J.O., Williams, C., Zhang, S., Milne, W.I., and Wilkinson, T.D. (2014). Plasmonic nanoparticle scattering for color holograms. PNAS *111*, 12679–12683.

Nassenstein, H. (1968). Holographie und interferenzversuche mit inhomogenen oberflächenwellen. Phys. Lett. A. *28*, 249–251.

Ni, X., Kildishev, A.V., and Shalaev, V.M. (2013). Metasurface holograms for visible light. Nat. Commun. *4*, 2807.

Nylander, C., Liedberg, B., and Lind, T. (1982). Gas detection by means of surface plasmon resonance. Sens. Actuators, A. *3*, 79–88.

Ono, A., Kato, J., and Kawata, S. (2005). Subwavelength optical imaging through a metallic nanorod array. Phys. Rev. Lett. *95*, 267407.

Otto, A. (1968). Excitation of nonradiative surface plasma waves in silver by the method of frustrated total reflection. Z. für Physik *216*, 398–410.

Ozaki, M., Kato, J., and Kawata, S. (2011). Surface-plasmon holography with white light illumination. Science *332*, 218–220.

Ozaki, M., Kato, J., and Kawata, S. (2012). Blur suppression in holographic imaging with use of surface plasmons. Appl. Phys. Lett. *101*, 241117.

Ozaki, M., Kato, J., and Kawata, S. (2013). Color selectivity of surface-plasmon holograms illuminated with white light. Appl. Opt. *52*, 6788–6791.

O'Neal, D.P., Hirsch, L.R., Halas, N.J., Payne, J.D., and West, J. (2004). Photo-thermal tumor ablation in mice using near infrared-absorbing nanoparticles. Cancer Lett. *209*, 171–176.

Raether, H. (1988). Surface Plasmons on Smooth and Rough Surfaces and on Gratings (Springer).

Sommerfeld, A. (1899). Ueber die Fortpflanzung elektrodynamischer Wellen längs eines Drahtes. Ann. D. Phys. *67*, 233–290.

Stetson, K.A. (1967). Holography with total internally reflected light. Appl. Phys. Lett. *11*, 225–226.

Stöckle, R.M., Suh, Y.D., Deckert, V., and Zenobi, R. (2000). Nanoscale chemical analysis by tip-enhanced Raman spectroscopy Chem. Phys. Lett. *318*, 131–136.

Sugiyama, M., Inasawa, S., Koda, S., Hirose, T., Yonekawa, T., Omatsu, T., and Takami, A. (2001). Optical recording media using laser-induced size reduction of Au nanoparticles. Appl. Phys. Lett. *79*, 1528–1530.

Suhara, T., Nishihara, H., and Koyama, J. (1976). Waveguide holograms: a new approach to hologram integration. Opt. Commun. *19*, 353–358.

Sun, Y., and Xia, Y. (2003). Gold and silver nanoparticles: a class of chromophores with colors tunable in the range from 400 to 750 nm. Analyst *128*, 686–691.

Takahara, J., Yamagishi, S., Taki, H., Morimoto, A., and Kobayashi, T. (1997). Guiding of a one-dimensional optical beam with nanometer diameter. Opt. Lett. *22*, 475–477.

Vaia, R.A., Dennis, C.L., Natarajan, L.V., Tondiglia, V.P., Tomlin, D.W., and Bunning, T.J. (2001). One-step, micrometer-scale organization of nano- and mesoparticles using holographic photopolymerization: a generic technique. Adv. Mater. *13*, 1570–1574.

Wang, G.P., Sugiura, T., and Kawata, S. (2001). Holography with surface-plasmon-coupled waveguide modes. Appl. Opt. *40*, 3649–3653.

Wheatstone, C. (1838). Contributions to the physiology of vision. –Part the first. On some remarkable and hitherto unobserved phenomena of binocular vision. Philos. Trans. R. Soc. *128*, 371–394.

Wood, R.W. (1902). On a remarkable case of uneven distribution of light in a diffraction grating spectrum. Phil. Mag. *4*, 396–402.

Yamaguchi, M., Sugiura, H., Honda, T., and Ohyama, N. (1992). Automatic recording method for holographic three-dimensional animation. J. Opt. Soc. Am. A. *9*, 1200–1205.

Yu, N., Genevet, P., Kats, M.A., Aieta, F., Tetienne, J.-P., Capasso, F., and Gaburro, Z. (2011). Light propagation with phase discontinuities: generalized laws of reflection and refraction. Science *334*, 333–337.

Smith, D.R., Pendry, J.B., and Wiltshire, M.C.K. (2004). Metamaterials and negative refractive index. Science *305*, 788–792.